

{Re^{III}Cl₃} Core Complexes with Bifunctional Single Amino Acid ChelatesSangeeta Ray Banerjee,[†] Lihui Wei,[†] Murali K. Levadala,[†] Neva Lazarova,[†] Vladimir O. Golub,[‡] Charles J. O'Connor,[‡] Karin A. Stephenson,[§] John F. Valliant,[§] John W. Babich,^{*||} and Jon Zubieta^{*†}*Department of Chemistry, Syracuse University, Syracuse, New York 13244, Biostream, Inc., 160 Second Street, Cambridge, Massachusetts 02142, Department of Chemistry, University of New Orleans, New Orleans, Louisiana 70148, and Department of Chemistry, McMaster University, Hamilton, ON L8S 4M1, Canada*

Received June 10, 2002

The reactions of the Re(V) starting material [ReO(PPh₃)₂Cl₃] with ligands of the type XN(Y)Z [X = Y = 2-pyridylmethyl, Z = -CH₂CO₂Et (L¹Et), -CH₂CH₂CO₂Et (L²Et), -CH₂CH₂CH₂CH₂CH(NHCO₂Bu)CO₂H (L³H); X = 2-pyridylmethyl, Y = 2-(1-methylimidazolyl)methyl, Z = -CH₂CO₂Et (L⁴Et)] yielded the Re(III) trichloride complexes of the type [ReCl₃(LⁿR)]. The complexes are mononuclear, paramagnetic species with a facial geometry of the chloride ligands. The nitrogen donors of the tridentate LⁿR ligands complete the distorted octahedral coordination spheres of the complexes. Crystal data: [ReCl₃(L¹Et)] (1), monoclinic, C2/m, a = 16.088(3) Å, b = 9.980(2) Å, c = 12.829(2) Å, β = 91.384(3)°, Z = 4, D_{calc} = 1.967 g/cm⁻³; [ReCl₃(L⁴Et)] (4), monoclinic, C2/c, a = 22.880(1) Å, b = 7.4926(4) Å, c = 22.560(1) Å, β = 94.186(1)°, Z = 8, D_{calc} = 2.001 g/cm⁻³.

The ability to incorporate readily available radionuclides with optimal decay characteristics into tracer molecules has been the foremost consideration in developing diagnostic radiopharmaceuticals. In this respect, ^{99m}Tc has become the mainstay of diagnostic nuclear medicine and in some chemical form is used in more than 85% of the diagnostic scans performed each year in hospitals.¹ This preferential use of ^{99m}Tc radiopharmaceuticals reflects the ideal nuclear properties of the isotope, as well as its convenient availability from commercial generator columns. ^{99m}Tc emits a 140 keV γ-ray with 89% abundance which is close to optimal for imaging with commercial γ cameras. The absence of tissue-damaging corpuscular radiation allows the injection of activities of more than 30 m Ci with low radiation exposure to the patient. The 6 h half-life is sufficiently long for

pharmaceutical preparation and in vivo accumulation in the target but yet short enough to minimize radiation dose to the patient or to cause environmental repercussions. Moreover, the availability of the relatively stable ⁹⁹Tc isomer allows development of technetium coordination chemistry and modeling of technetium radiopharmaceuticals.² Radiopharmaceuticals may be classified into two broad categories: (i) those with biological distribution determined strictly by blood flow, or perfusion, and targeting high-capacity systems such as glomerular filtration, phagocytosis, hepatocyte clearance, and bone absorption; (ii) those whose distribution is determined by specific enzymatic or receptor binding interactions and which target low-capacity sites.¹ The latter approach has adopted two methods to chelate ^{99m}Tc in a receptor specific molecule.³ The conjugate or pendant method involves tethering a ^{99m}Tc chelate moiety to a species known to possess high-affinity binding to a receptor. The integrated approach replaces a portion of the high-affinity receptor ligand with a ^{99m}Tc chelate, so as to preserve the binding affinity, a methodology which has been most convincingly exploited by Katzenellenbogen in the imaging of the estrogen receptor sites of tumor cells.⁴

* To whom correspondence should be addressed. E-mail: jazubiet@syr.edu.

† Syracuse University.

‡ University of New Orleans.

§ McMaster University.

|| Biostream, Inc.

- (1) Recent reviews include: (a) Nicolini, M.; Bandoli, G.; Mazzi, U., Eds. *Technetium, Rhenium and Other Metals in Chemistry and Nuclear Medicine*, 5; Raven Press: New York, 2000. (b) Nicolini, M.; Bandoli, G.; Mazzi, U., Eds. *Technetium and Rhenium in Chemistry and Nuclear Medicine*; Raven Press: New York, 1990. (c) Jurisson, S. S.; Lyden, J. D. *Chem. Rev.* **1999**, *99*, 2205. (d) Liu, S.; Edwards, O. S. *Chem. Rev.* **1999**, *99*, 2235. (e) Dilworth, J. R.; Parrott, S. J. *Chem. Soc. Rev.* **1998**, *27*, 43. (f) Hom, R. K.; Katzenellenbogen, J. A. *Nucl. Med. Biol.* **1997**, *24*, 485. (g) Eckelman, W. C. *Eur. J. Nucl. Med.* **1995**, *22*, 249. (h) Schwochan, K. *Angew. Chem., Int. Ed. Engl.* **1994**, *33*, 2258.

- (2) See, for example: (a) Liu, S.; Edwards, D. S.; Harris, A. R.; Hemingway, S. J.; Barrett, J. F. *Inorg. Chem.* **1999**, *38*, 1326. (b) Bandoli, G.; Dolmella, A.; Porchea, M.; Refosco, F.; Tisato, F. *Coord. Chem. Rev.* **2001**, *241*, 43. (c) Rose, D. J.; Maresca, K. P.; Nicholson, T.; Davison, A.; Jones, A. G.; Babich, J.; Fischman, A.; Graham, W.; DeBord, J. R. D.; Zubieta, J. *Inorg. Chem.* **1998**, *37*, 2701 and references therein.

Our efforts⁵ have concentrated on the pendant approach which requires several components: a high-affinity receptor ligand on the targeting molecule; a bifunctional chelator for the conjugation of the receptor ligand and the coordination of the radionuclide, ^{99m}Tc. While a variety of biologically active molecules have been exploited as the carriers for the radionuclide–ligand subunit, small peptides offer significant advantages compared to antibodies or proteins.⁶ Peptides are necessary elements in a greater variety of fundamental biological processes than other biomolecules, and their affinities for their receptors can be significantly greater than those of macromolecules. Small peptides also exhibit smaller size and enhanced diffusibility into the extravascular space, faster blood clearance resulting in lower background radiation, and the presence of well-defined receptor systems. Furthermore, analogues of these peptides with varying size, charge, and linker properties are readily prepared.⁷

The second component, the “bifunctional” ligand, serves two purposes: to hold the metal radionuclide securely without loss in vivo; to provide a pendant arm for peptide linkage while maintaining maximal biomolecule integrity. Thus, the terminus that chelates the technetium must possess the greatest attainable thermodynamic and kinetic stability under biological conditions, while the second terminus of the bifunctional chelate forms a covalent bond to the biological molecule. Furthermore, bifunctional chelators must be capable of conjugation under mild, aqueous conditions reasonably close to physiological pH, in a relatively short time, with minimal need for purification procedures. Of course in the most general case, the “bifunctional” subunit consists of a linker functionality (C), a set of functional donor groups (A), and a tethering moiety (B), which may also include additional functional groups (Chart 1).

We have recently initiated the development of a family of bifunctional chelators based on pyridyl-, imidazole-, and/or carboxylate-derivatized amino acids or diamino diacids for conjugation to small peptides by solid-phase synthetic methods⁷ or to other biomolecules by more conventional strategies. To achieve this, lysine, alanine, glycine, and a series of bis(amino acids) have been modified to incorporate a tridentate chelation terminus (A) as well as a

Chart 1

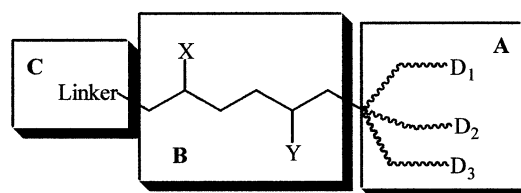


Chart 2

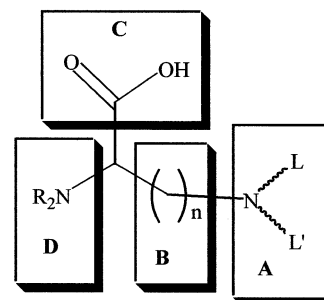
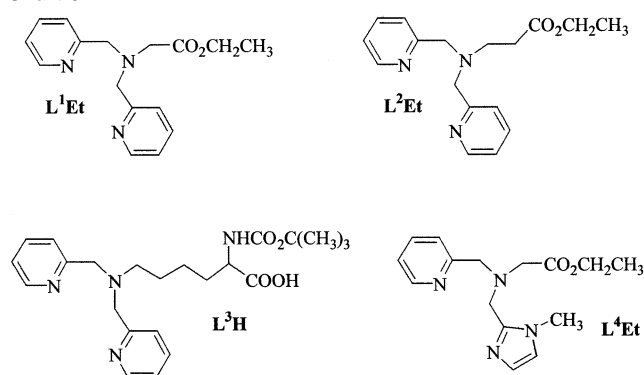


Chart 3



terminus (C) for conjugation to small peptides exploiting solid-phase synthesis. The tether unit B is variable in length and may also be functionalized. The amino unit of the parent amino acid may also be derivatized, providing additional versatility (Chart 2). The ligands of this study shown in Chart 3 are derived from glycine, β -alanine, and lysine as representative examples to demonstrate the feasibility of the approach.

While our focus has been on donor sets appropriate for the $\{M(CO)_3\}^+$ ($M = Tc, Re$) core, we have also investigated the coordination chemistry of these ligand types with other rhenium and technetium core structures. As part of this continuing investigation, we report the synthesis and properties of a series of Re(III) complexes of the general type $[ReCl_3\{XN(Y)Z\}]$, where $\{XN(Y)Z\}$ is a tridentate ligand constructed from an amino acid. The structure of two derivatives are described, $[ReCl_3(L^1Et)]$ (1) and $[ReCl_3(L^4Et)]$ (4), where $L^1Et = (2-C_5H_4NCH_2)_2NCH_2CO_2C_2H_5$ and $L^4Et = (2-C_5H_4NCH_2)N(CH_3C_3H_7N_2CH_2)(CH_2CO_2C_2H_5)$.

- (3) (a) Yeh, W. M.; Sherman, D. G.; Meares, C. F. *Anal. Chem.* **1979**, *100*, 152. (b) Meares, C. F.; Wensel, T. G. *Acc. Chem. Res.* **1984**, *17*, 202. (c) Meares, C. F. In *Protein Tailoring for Food and Medical Uses*; Feeney R. E., Whitaker, J. R., Eds.; Marcel Dekker: New York, 1986; p 339. (d) Brechbiel, M. W.; Gansow, O. A.; Atcher, R. W.; Schlom, J.; Esteban, J.; Simpson, D. E.; Colcher, D. *Inorg. Chem.* **1986**, *25*, 2772 and references therein. (e) Hnatowich, D. J.; Mardirossian, A.; Ruscowski, M.; Fargarasi, M.; Firji, F.; Winnard, P. *J. Nucl. Med. Chem.* **1993**, *34*, 772.
- (4) Shadden, M. B.; Wüst, F. R.; Jonson, S.; Syhre, R.; Welch, M. J.; Spies, H.; Katzenellenbogen, J. A. *Nucl. Med. Biol.* **2000**, *27*, 269 and references therein.
- (5) (a) Babich, J. W.; Graham, W.; Femia, F. J.; Dong, Q.; Barzana, M.; Ferrill, K.; Fischman, A. J.; Zubietta, J. *Inorg. Chim. Acta* **2001**, *323*, 23. (b) Babich, J. W.; Coco, W. G.; Barrow, S.; Fischman, A. J.; Femia, F. J.; Zubietta, J. *Inorg. Chim. Acta* **2000**, *309*, 123. (c) Rose, D. J.; Maresca, K. P.; Nicholson, T.; Davison, A.; Jones, A. G.; Babich, J. W.; Fischman, A.; Graham, W.; DeBord, J. R. D.; Zubietta, J. *Inorg. Chem.* **1998**, *37*, 2701. (d) Schwartz, D. A.; Abrams, M. J.; Hauser, M. M.; Gaul, F. E.; Larsen, S. K.; Rauth, D.; Zubietta, J. *Bioconjugate Chem.* **1991**, *2*, 333.
- (6) Liu, S.; Edwards, D. S.; Barrett, J. A. *Bioconjugate Chem.* **1997**, *8*, 621.

- (7) (a) Aimoto, S. Contemporary methods for peptide synthesis. *Curr. Org. Chem.* **2001**, *5*, 45–87 and references therein. (b) Gausepohl, H.; Behn, C. Automated peptide synthesis, cleavage and purification. In *Innovation and Perspectives in Solid Phase Synthesis, Collected Papers*, 3rd International Symposium, 1994; Mayflower Worldwide Ltd.: Birmingham, U.K.; and references therein. (c) Atherton, E.; Sheppard, R. C., *Solid Phase Peptide Synthesis*; IRC Press: Oxford, U.K., 1989. (d) Barrett, G. C.; Elmore, D. T. *Amino Acids and Peptides*; Cambridge University Press: Cambridge, U.K., 1998.

Experimental Section

General Methods. All reagents and organic solvents used in this study are reagent grade and were used without further purification. $[ReOCl_3(PPh_3)_2]$ was prepared according to the literature method.⁸ Acetonitrile used for electrochemical experiments was dried by passing through a alumina column just before the experiments. 1H and ^{13}C NMR spectra were recorded on a Bruker DPX 300 spectrometer; all peak positions are relative to TMS. IR spectra were recorded as KBr pellets with a Perkin-Elmer Series 1600 FT-IR spectrometer in the range 400–4000 cm^{-1} with polystyrene as reference. Electrospray mass spectrometry (ESMS) was performed on a Fisons Platform quadrupole instrument where samples were dissolved in 50:50 CH_3CN/H_2O . For compounds analyzed in the positive ion mode, one drop of 0.1% trifluoroacetic acid was added. For compounds run in negative mode, one drop of 0.10 M NH_4OH was added. Carbon, hydrogen, and nitrogen analyses were carried out by Oneida research services, Whitesboro, NY. A BAS potentiostat (model CV-27) equipped with data-collecting and analyzing capabilities was used for the electrochemical experiments. Dry acetonitrile, deoxygenated under a dinitrogen atmosphere, was used as the solvent. Solutions were 0.1 M in tetra-*n*-butylammonium hexafluorophosphate, TBAH ($[NBu_4]PF_6$), as supporting electrolyte. A three-compartment glass cell equipped with a platinum bead as the working electrode, a platinum wire as the counter electrode, and a silver wire as the pseudoreference electrode was used for all experiments. $E_{1/2}$ values determined as $(E_{p,a} + E_{p,c})/2$ are uncorrected for junction potentials. Under our experimental conditions (sweep rate: 100 $mV s^{-1}$) the ferrocenium/ferrocene couple is at $E_{1/2} = +0.18$ V, and we have used bis(cyclopentadienyl)cobalt(III) hexafluorophosphate as an internal standard, $E_{1/2} = -1.15$ V, with respect to the ferrocenium/ferrocene couple under the same experimental conditions.

Ligand Syntheses. Ethyl (Bis(2-pyridylmethyl)amino)acetate (L¹Et). The synthesis of the ligand involves two steps. Step 1 is the synthesis of (bis(2-pyridylmethyl)amino)acetic acid (L¹H). The following procedure is based on literature procedures⁹ with slight modifications. 2-(Chloromethyl)pyridine hydrochloride (9.2 g, 56.0 mmol) and glycine (2 g, 26.6 mmol) were dissolved in water (30 mL) and stirred at room temperature for 5 days, with addition of 5 $mol dm^{-3}$ aqueous NaOH solution at intervals to maintain the pH at 8–10. The resulting dark red solution was extracted with ethyl acetate, and then the aqueous phase was acidified to pH 6, extracted with chloroform, and concentrated. Pale yellow crystals of the pure ligand were obtained from dichloromethane. Yield: 2.87 g (11.2 mmol, 42%). 1H NMR (δ (ppm), CD_3OD): 8.29 (d, $J = 5.1$ Hz, 2H, PyH), 7.60 (t, $J = 9.0$ Hz, 2H, PyH), 7.30 (d, $J = 7.8$ Hz, 2H, PyH), 7.12 (t, $J = 6.2$ Hz, 2H, PyH), 4.10 (s, 4H, $PyCH_2$), 3.39 (s, 2H, NCH_2). ^{13}C NMR (CD_3OD , 300 MHz): δ 173.05 (C, CO_2H), 156.10 (2C, Py), 149.76 (2CH, Py), 139.31 (2CH, Py), 125.15 (2CH, Py), 124.77 (2CH, Py), 59.77 (2C, $PyCH_2$), 57.77 (C, NCH_2). Step 2 is esterification of (bis(2-pyridylmethyl)amino)acetic acid. (Bis(2-pyridylmethyl)amino)acetic acid (L¹H) (1 g, 3.89 mmol) was dissolved in saturated ethanolic HCl (20 mL) and refluxed for 3 h. The reaction mixture was quenched with triethylamine and concentrated. The residue was dissolved in dichloromethane, washed with water, dried (Na_2SO_4), and concentrated. The residue was purified by silica gel column chromatography using methanol/chloroform (3:97) to give ethyl (bis(2-pyridylmethyl)amino)acetate (L¹Et) as a viscous liquid. Yield: 910 mg (3.19 mmol, 82%). 1H

NMR (δ (ppm), $CDCl_3$): 8.49 (d, $J = 3.0$ Hz, 2H, PyH), 7.96 (t, $J = 4.2$ Hz, 2H, PyH), 7.53 (d, $J = 7.8$, 2H, PyH), 7.12 (t, $J = 5.7$, 2H, PyH), 3.97 (s, 4H, $PyCH_2$), 3.42 (s, 2H, NCH_2), 4.12 (q, 2H, OCH_2), 1.22 (s, 3H, CH_3). ^{13}C NMR ($CDCl_3$): δ 171.05 (C, CO_2R), 158.80 (2C, Py), 148.80 (2CH, Py), 136.32 (2CH, Py), 122.93 (2CH, Py), 121.88 (2CH, Py), 59.70 (2C, CH_2Py), 54.67 (C, NCH_2), 60.21 (OCH_2), 13.99 (CH_3).

Ethyl 3-(Bis(2-pyridylmethyl)amino)propionate (L²Et). The ligand synthesis involves two steps. Step 1 is the synthesis of 3-(bis(2-pyridylmethyl)amino)propionic acid (L²H). This compound was synthesized by a procedure similar to that described as above in the case of L¹H, except that 3-aminopropionic acid used instead of glycine. From 7.73 g (47.2 mmol) of 2-(chloromethyl)pyridine hydrochloride and 2 g (22.4 mmol) of 3-aminopropionic acid, pale-red crystals of 3-(bis(2-pyridylmethyl)amino)propionic acid formed in dichloromethane and were collected and dried under vacuum. Yield: 2.74 g (10.1 mmol, 45%). 1H NMR (δ (ppm), CD_3OD): 8.40 (d, $J = 5.1$ Hz, 2H, PyH), 7.73 (t, $J = 9.0$ Hz, 2H, PyH), 7.51 (d, $J = 7.8$ Hz, 2H, PyH), 7.24 (t, $J = 6.0$ Hz, 2H, PyH), 3.93 (s, 4H, $PyCH_2$), 2.96 (t, $J = 6.9$ Hz, 2H, NCH_2), 2.5 (t, $J = 6.9$ Hz, 2H, CH_2CO_2). ^{13}C NMR (CD_3OD): δ 176.79 (C, CO_2H), 158.20 (2C, Py), 149.72 (2CH, Py), 138.98 (2CH, Py), 125.29 (2CH, Py), 124.37 (2CH, Py), 60.22 (2C, $PyCH_2$), 51.90 (C, NCH_2), 33.15 (C, CH_2). Step 2 for the esterification of 3-(bis(2-pyridylmethyl)amino)propionic acid was carried out under conditions similar to those used for L¹Et. Purification was effected by silica gel column chromatography using methanol/chloroform (3:97) to give ethyl 3-(bis(2-pyridylmethyl)amino)propionate as a viscous liquid. Yield: 1.37 g (4.59 mmol, 83%). 1H NMR (δ (ppm), $CDCl_3$): 8.48 (d, $J = 5.1$ Hz, 2H, PyH), 7.51 (t, $J = 4.28$ Hz, 2H, PyH), 7.39 (d, $J = 6.0$ Hz, 2H, PyH), 7.03 (t, $J = 6.1$ Hz, 2H, PyH), 3.74 (s, 4H, $PyCH_2$), 2.84 (t, $J = 6.1$ Hz, 2H, NCH_2), 2.45 (t, $J = 6.1$ Hz, 2H, CH_2CO), 3.98 (q, OCH_2), 1.09 (t, $J = 6.2$ Hz, CH_3). ^{13}C NMR ($CDCl_3$): δ 171.74 (C, CO_2R), 158.91 (2C, Py), 148.40 (2CH, Py), 135.82 (2CH, Py), 122.42 (2CH, Py), 121.47 (2CH, Py), 59.39 (2C, $PyCH_2$), 49.32 (C, NCH_2), 33.15 (C, CH_2), 59.55 (OCH_2), 13.70 (CH_3).

Preparation of *N*- α -(*tert*-butoxycarbonyl)-*N*- ω -bis(2-pyridylmethyl)-L-lysine (L³H). The compound was prepared using procedures analogous to that described for L¹H. The crude product was purified by column chromatography using 10% chloroform in methanol to give *N*- α -(*tert*-butoxycarbonyl)-*N*- ω -bis(2-pyridylmethyl)-L-lysine (L³H) as a red viscous liquid (950 mg, 55%). 1H NMR (δ , CD_3OD): 8.78 (d, $J = 5.1$ Hz, 2H, PyH), 8.50 (t, $J = 7.5$ Hz, PyH), 8.08 (d, $J = 7.8$ Hz, 2H, PyH), 7.93 (t, $J = 6.3$ Hz, 2H, PyH), 4.24 (t, H, $NCHCO_2$), 3.86 (s, 4H, $PyCH_2$), 2.57 (t, 2H, NCH_2), 1.62–1.26 (m, 6H, CH_2), 1.41 (s, 9H, tBu). ^{13}C NMR (CD_3OD): δ 177.49 (C, CO_2H), 157.71 (2C, Py), 149.72 (2CH, PyH), 138.93 (2CH, Py), 125.11 (2CH, Py), 124.34 (2CH, Py), 80.06 (CH, NCH), 60.12 (2C, $PyCH_2$), 55.50 (C, NCH_2), 33.15 (C, CH_2), 28.93 (3C, tBu), 26.66 (C, CH_2), 24.31 (C, CH_2).

Ethyl [(2-pyridylmethyl)((1-methylimidazol-2-yl)methyl)amino]acetate (L⁴Et). A solution of 1-methylimidazole-2-aldehyde (5 g, 45.1 mmol) in 100 mL of methanol was added slowly to 2-picolyamine (94.88 g, 45.1 mmol), and the solution was stirred for 2 h. At this time, the reactants were completely consumed. To this reaction mixture was added $NaBH_4$ (1.7 g, 45.1 mmol) in portions, and the solution was stirred for another 3 h, whereupon the solution was evaporated to dryness and the residue was extracted with chloroform and concentrated. This residue was dissolved in anhydrous dimethylformamide (40 mL). Potassium carbonate (97.53 g, 45.1 mmol) and ethyl bromoacetate (96.23 g, 45.1 mmol) were added to the solution under argon atmosphere. The resulting

(8) (a) Parshall G. W. *Inorg. Synth.* **1977**, *17*, 110. (b) Chatt, J.; Row, G. A. *J. Chem. Soc.* **1962**, 4019.

(9) Iikura, H.; Nagata, T. *Inorg. Chem.* **1998**, *37*, 4702.

suspension was protected from light and allowed to stir at 30 °C, under argon, for 32 h. The reaction mixture was filtered, and the filtrate was evaporated to dryness. The resulting red oil was purified by chromatography using a 95:5 chloroform/methanol solution to give 7.80 g of the product. Yield: 60%. ¹H NMR (δ, ppm, CD₃OD): 8.33 (d, *J* = 3.1 Hz, 1H, PyH), 7.73 (t, *J* = 5.8 Hz, 1H, PyH), 7.36 (d, *J* = 6.0, 1H, PyH), 7.18 (t, *J* = 6.1, 1H, PyH), 6.80 (d, 1H, ImH), 6.71 (d, 1H, ImH), 3.86 (s, 2H, PyCH₂), 3.83 (s, 2H, ImCH₂), 3.58 (s, 2H, NCH₂), 3.22 (s, 3H, NCH₃), 3.97 (q, OCH₂), 1.13 (t, *J* = 6.2, CH₃). ¹³C NMR (CD₃OD): δ 172.23 (C, CO₂H), 159.93 (C, Py), 149.72 (CH, Py), 146.26 (C, Im), 138.69 (C, PyH), 127.22 (C, PyH), 125.01 (C, PyH), 123.99 (CH, Im), 123.71 (CH, Im), 60.66 (C, PyCH₂), 55.54 (C, ImCH₂), 51.39 (C, NCH₂), 33.56 (C, NCH₃), 61.62 (C, OCH₂), 14.73 (C, CH₃).

Synthesis of the Complexes of the Type [ReCl₃(L)] (1–4). The complexes were prepared by following the general procedure described for **1**.

[ReCl₃(L¹Et)] (1). To a stirred solution of [ReOCl₃(PPh₃)₂] (0.2 g, 0.24 mmol) in 15 mL of chloroform was added L¹Et (0.08 g, 0.28 mmol) in 5 mL of chloroform. The solution was refluxed for 2 h, whereupon the reaction mixture became dark brown-red. Upon cooling, a deep red precipitate formed, which was collected by filtration and washed several times with ether and hexane and finally with a small amount of dichloromethane. Yield: 0.1 g (87%). An additional product was recovered from the filtrate. The overall yield was nearly quantitative. Anal. Calcd (found) for C₁₆H₁₉O-Cl₃N₃O₂Re: C, 33.89 (33.25); H, 3.44 (3.31); N, 6.99 (7.27).

IR (KBr/cm⁻¹): 1730 (ν_{as}(C=O)), 1208 (ν_{sym}(C=O)) of the ester part of ligand. CV (*E*_{1/2} (Δ*E*, mV)) (acetonitrile/(TBA)PF₆/100 mV s⁻¹): *E*_{1/2}(IV/III) = +0.021 V (60); *E*_{1/2}(III/II) = -1.414 V (60).

[ReCl₃(L²Et)] (2). Yield: 70%. Anal. Calcd (found) for C₁₇H₂₁-Cl₃N₃O₂Re: C, 34.21 (34.49); H, 3.44 (3.57), N, 6.83 (7.09). IR (KBr/cm⁻¹): 1720 (ν_{as}(C=O)), 1195 (ν_{sym}(C=O)) of the ester part of ligand. CV (*E*_{1/2} (Δ*E*, mV)): *E*_{1/2}(IV/III) = -0.046 V (60); *E*_{1/2}(III/II) = -1.47 V (60).

[ReCl₃(L³Et)] (3). Yield: 60%. Anal. Calcd for C₂₃H₃₂Cl₃N₄-O₄Re: C, 38.75 (38.28); H, 3.31 (3.21), N, 7.53 (7.77). IR (KBr/cm⁻¹): 1734 (ν_{as}(C=O)), 1190 (ν_{sym}(C=O)) of the ester part of ligand. CV (*E*_{1/2} (Δ*E*, mV)): *E*_{1/2}(IV/III) = -0.107 V (80); *E*_{1/2}(III/II) = -1.51 V (82).

[ReCl₃(L⁴Et)] (4). Yield: 56%. Anal. Calcd (found) for C₁₅H₂₀-Cl₃N₄O₂Re: C, 31.21 (31.01); H, 3.57 (3.45); N, 9.70 (9.65). IR (KBr/cm⁻¹): 1720 (ν_{as}(C=O)), 1210 (ν_{sym}(C=O)) of the ester part of ligand. CV (*E*_{1/2} (Δ*E*, mV)): *E*_{1/2}(IV/III) = -0.198 V (60); *E*_{1/2}(III/II) = -1.71 V (60).

[Re(NCS)₃(L¹Et)] (5). To a stirred solution of [Re(Cl)₃(L¹Et)] (**1**) (0.11 g, 0.17 mmol) in 15 mL of acetonitrile was added 0.053 g (0.55 mmol) of KSCN in 5 mL of acetonitrile. The solution was refluxed for 5 h. The color of the reaction mixture changed from red to golden yellow. The reaction mixture was cooled and filtered to remove the KCl precipitate. After stripping of the solvent under reduced pressure, the residue was dissolved in chloroform and purified by column chromatography using a silica gel column. The golden yellow band of the pure complex was eluted with a 5% methanol/chloroform mixture. A yellow microcrystalline precipitate was directly obtained from the eluted solution of the complex upon slow evaporation at room temperature. Yield: 0.08 g (70%). IR (KBr/cm⁻¹): 2048, 1996 (ν(NCS)); 1745 (ν_{as}(C=O)), 1202 (ν_{sym}(C=O)) of the ester part of ligand.

X-ray Crystal Structure Determinations of 1 and 4. The selected crystals of **1** and **4** were studied on a Bruker diffractometer

Table 1. Crystal Data for [ReCl₃(L¹Et)] (**1**) and [ReCl₃(L⁴Et)] (**4**)

param	1	4
formula	C ₁₇ H ₂₃ Cl ₃ N ₃ O ₃ Re	C ₁₅ H ₂₀ Cl ₃ N ₄ O ₂ Re
fw	609.93	580.90
space group	C2/m	C2/c
<i>T</i> , K	293(2)	90(2)
<i>a</i> , Å	16.088(3)	22.880(1)
<i>b</i> , Å	9.980(2)	7.4926(4)
<i>c</i> , Å	12.829(2)	22.560(1)
β, deg	91.384(3)	94.186(1)
<i>V</i> , Å ³	2059.2(6)	3857.2(4)
<i>Z</i>	4	8
<i>D</i> _{calc} , g cm ⁻³	1.967	2.001
μ, mm ⁻¹	6.313	6.733
R1 ^a	0.0442	0.0715
wR2 ^a	0.1135	0.1178

$$^a R1 = \sum ||F_o| - |F_c|| / \sum |F_o|; wR2 = [\sum w(F_o^2 - F_c^2)^2 / \sum w(F_o^2)^2]^{1/2}.$$

Table 2. Selected Bond Lengths (Å) and Angles (deg) for [ReCl₃(L¹Et)] (**1**) and [ReCl₃(L⁴Et)] (**4**)^a

1		4	
Re(1)–N(2)	2.075(9)	Re(1)–N(1)	2.078(6)
Re(1)–N(2) ^{#1}	2.075(9)	Re(1)–N(2)	2.084(5)
Re(1)–N(1)	2.154(14)	Re(1)–N(4)	2.209(5)
Re(1)–Cl(1) ^{#1}	2.384(3)	Re(1)–Cl(1)	2.3741(17)
Re(1)–Cl(1)	2.384(3)	Re(1)–Cl(2)	2.3996(16)
Re(1)–Cl(2)	2.391(4)	Re(1)–Cl(3)	2.4040(17)
N(2)–Re(1)–N(2) ^{#1}	82.1(6)	N(1)–Re(1)–N(2)	83.9(20)
N(2)–Re(1)–N(1)	80.4(4)	N(1)–Re(1)–N(4)	78.8(2)
N(2) ^{#1} –Re(1)–N(1)	80.4(4)	N(2)–Re(1)–N(4)	80.94(18)
N(2)–Re(1)–Cl(1) ^{#1}	91.6(3)	N(1)–Re(1)–Cl(1)	95.29(16)
N(2) ^{#1} –Re(1)–Cl(1) ^{#1}	171.1(3)	N(2)–Re(1)–Cl(1)	93.08(14)
N(1)–Re(1)–Cl(1) ^{#1}	92.5(2)	N(4)–Re(1)–Cl(1)	171.94(14)
N(2)–Re(1)–Cl(1)	171.1(3)	N(1)–Re(1)–Cl(2)	91.90(15)
N(2) ^{#1} –Re(1)–Cl(1)	91.6(3)	N(2)–Re(1)–Cl(2)	172.09(14)
N(1)–Re(1)–Cl(1)	92.5(2)	N(4)–Re(1)–Cl(2)	91.69(13)
Cl(1) ^{#1} –Re(1)–Cl(1)	93.86(15)	Cl(1)–Re(1)–Cl(2)	93.97(6)
N(2)–Re(1)–Cl(2)	94.6(3)	N(1)–Re(1)–Cl(3)	171.28(16)
N(2) ^{#1} –Re(1)–Cl(2)	94.6(3)	N(2)–Re(1)–Cl(3)	90.16(14)
N(1)–Re(1)–Cl(2)	173.2(3)	N(4)–Re(1)–Cl(3)	94.03(14)
Cl(1) ^{#1} –Re(1)–Cl(2)	92.13(9)	Cl(1)–Re(1)–Cl(3)	91.37(7)
Cl(1)–Re(1)–Cl(2)	92.13(9)	Cl(2)–Re(1)–Cl(3)	93.25(6)

^a Symmetry transformations used to generate equivalent atoms: #1, *x*, -*y* + 1, *z*.

equipped with the SMART CCD system,¹⁰ using graphite-monochromated Mo Kα radiation (λ = 0.710 73 Å). The data collection was carried out at 89(5) K. The data were corrected for Lorentz polarization effects, and absorption corrections were made using SADABS.¹¹ All calculations were performed using SHELXTL.¹² The structures were solved by direct methods, and all of the non-hydrogen atoms were located from the initial solution. After location of all the non-hydrogen atoms in the structure, the model was refined against *F*², initially using isotropic and later anisotropic thermal displacement parameters until the final value of Δ/*σ*_{max} was less than 0.001. At this point the hydrogen atoms were located from the electron density difference map and a final cycle of refinements was performed, until the final value of Δ/*σ*_{max} was again less than 0.001. No anomalies were encountered in the refinement of the structure. The relevant parameters for crystal data, data collection, structure solution, and refinement are summarized in Table 1, and important bond lengths and bond angles are in Table 2. A complete

(10) SMART Software Reference Manual; Siemens Analytical X-ray Instruments, Inc.: Madison, WI, 1994.

(11) Sheldrick, G. M. SADABS: Program for Empirical Absorption Corrections; University of Göttingen: Göttingen, Germany, 1996.

(12) Sheldrick, G. M. SHELXL96: Program for Refinement of Crystal Structures; University of Göttingen: Göttingen, Germany, 1996.

description of the details of the crystallographic methods is given in the Supporting Information.

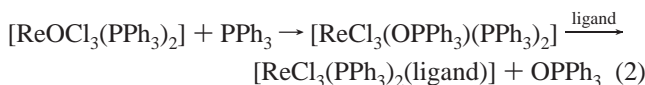
Magnetic Studies. The magnetic data were recorded on a 19.8 mg polycrystalline sample of **1** in the 2–350 K temperature range using a Quantum Design MPMS-5S SQUID spectrometer. Calibrating and operating procedures have been reported elsewhere.¹³ The temperature-dependent magnetic data were obtained at magnetic fields of $H = 500, 1000,$ and $10\,000$ Oe. The dependence of magnetization on magnetic field was recorded at 10 and 200 K.

Results and Discussion

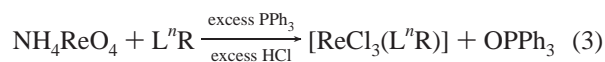
Syntheses and Properties. The rhenium complexes **1–4** were prepared as red crystals in good yields by treating $[ReOCl_3(PPh_3)_2]$ with the appropriate ligand in refluxing chloroform, according to the equation



The reduction of the $\{Re^VO\}^{3+}$ core of the starting material to the $\{Re^{III}Cl_3\}$ unit of the product is effected through phosphine abstraction of the oxo group, to form $OPPh_3$ as a byproduct. While there are previously reported examples of Re(III) trichloride complexes prepared directly from $[ReOCl_3(PPh_3)_2]$, it is generally necessary to employ additional PPh_3 to abstract the oxo group and reduce the Re(V) of the starting material,¹⁴ according to



However, the tridentate nitrogen donors of this study effect the direct and facile substitution of the oxo group and the phosphine ligands to give product in good yield. Moreover, the syntheses of **1–4** can be regarded as a good example of ligand-induced geometrical rearrangement since the starting material $[ReOCl_3(PPh_3)_2]$ exhibits the *mer*-trichloro geometry around the rhenium center, while the complexes **1–4** are *fac*-trichloro species, as confirmed by X-ray crystal structure analysis. The compounds may also be prepared from NH_4ReO_4 in the presence of PPh_3 as reductant and excess HCl:



Replacement of the ester substituent of the ligand with an aliphatic group, as in $(2-C_5H_4NCH_2)_2NC_2H_5$, resulted in intractable mixtures, suggesting that the electron-withdrawing ester group is required for reactivity. It is noteworthy that the reaction of ethyl bis(2-(1-methylimidazolyl)aminoacetate with $[ReOCl_3(PPh_3)_2]$ fails to provide complexes of the $[ReCl_3(L^nR)]$ type. Similarly, reaction of bis(2-pyridylmethyl)amine with this starting material provides a transient product which is unstable under the conditions of synthesis. These observations suggest that the smooth reaction of the Re(V) oxo precursor to yield the Re(III) trichloro products is highly sensitive to the ligand electronic structure, as

manifested both in the nature of the donor groups and the identity of the pendant.

Several examples of the coordination chemistry of Re with tridentate nitrogen donor ligands have been described in recent years. These include the Re(V) oxo core $\{ReO\}^{3+}$ complexes $[ReO(OCH_2CH_2O)(tpa)]PF_6$ ¹⁵ [$tpa = \text{tris}(2\text{-pyridylmethyl)amine}$], $[ReO(OCH_2CH_2O)(Bpz_4)]$ [$Bpz_4 = \text{tetrakis}(\text{pyrazol-1-yl})\text{borate}$],¹⁶ and $[ReO(C_2O_4)(HBpz_3)]$ ($HBpz_3 = \text{hydridotris}(1\text{-pyrazolyl})\text{borato}$).¹⁷ Low-valent complexes include the Re(III) species $[ReCl_2(tpa)]PF_6$,¹⁸ $[Re(\text{terpyridyl})_2Cl](PF_6)_2$,¹⁹ and $[Re(\text{terpyridyl})Cl_3]$.²⁰ While the latter complex $[Re(\text{terpyridyl})Cl_3]$ exhibits a $\{ReN_3Cl_3\}$ coordination stoichiometry analogous to that the compounds of this study, the geometric constraints of the terpyridine ligand dictate that $[Re(\text{terpyridyl})Cl_3]$ adopt a meridional ligand geometry rather than the facial geometry of the complexes **1–5**. While the coordination chemistry of Re(III) is dominated by the diamagnetic, binuclear Re_2^{6+} core,²¹ other examples of Re(III) monomers, exhibiting octahedral coordination and paramagnetism, have also been described. Many representative examples contain nitrogen donor ligands and are neutral species,^{22–26} although cationic chloro complexes with phosphine ligands have also been reported.

The complexes **1–4** undergo facile substitution reactions at the chloride sites. Compound **1** reacted rapidly with KSCN to yield $[Re(NCS)_3(L^1Et)]$ (**5**) in good yield. The infrared spectrum exhibits strong CN stretching modes from thiocyanate $\nu(C\equiv N)$ at 2048 and 1996 cm^{-1} , frequencies which suggest that the thiocyanate groups are N-bound.^{27,28} The electrospray mass spectrum of **5** displayed a highest m/z peak at 645, unambiguously assigned to the $[Re(NCS)_3(L^1Et)]^+$ parent ion on the basis of the isotopic distributions of ^{185,187}Re. Similarly, the electrospray MS of the compound **1** displayed the highest m/z peak at 591, consistent with the $[ReCl_3(L^1Et)]^+$ parent ion.

The paramagnetism of **1** is confirmed by NMR and magnetic susceptibility studies. As shown in Figure 1, the compound does not exhibit Curie–Weiss behavior up to 350 K. Analysis of the dependence of $\chi(H)$ on T provides a temperature-independent paramagnetic susceptibility of ca. 10^{-3} emu Oe⁻¹ mol⁻¹. While the weak variation of susceptibility with temperature can be ascribed to strong anisotropy,

- (15) Sugimoto, H.; Sasaki, Y. *Chem. Lett.* **1997**, 541.
 (16) Paulo, A.; Domingos, A.; Pires de Matos, A.; Santos, I.; Carvalho, M. F. N. N.; Pombiero, A. J. L. *Inorg. Chem.* **1994**, 33, 4729.
 (17) Brown, S. N.; Mayer, J. M. *Inorg. Chem.* **1992**, 31, 4091.
 (18) Helberg, L. E.; Orth, S. P.; Sabat, M.; Harman, W. D. *Inorg. Chem.* **1996**, 35, 5584.
 (19) Rall, J.; Weingart, F.; Ho, D. M.; Heeg, M. J.; Tisato, F.; Deutsch, E. *Inorg. Chem.* **1994**, 33, 3442.
 (20) Helberg, L. E.; Barrera, J.; Sabat, M.; Harman, W. D. *Inorg. Chem.* **1995**, 34, 2033.
 (21) Cotton, F. A. *Inorg. Chem.* **1998**, 37, 5710.
 (22) Fortin, S.; Beauchamp, A. L. *Inorg. Chem.* **2001**, 40, 105 and references therein.
 (23) Pearson, C.; Beauchamp, A. L. *Inorg. Chem.* **1998**, 37, 1242.
 (24) Bertolasi, V.; Marchi, A.; Marvelli, L.; Rossi, R.; Bianchini, C.; de los Rios, I.; Peruzzini, M. *Inorg. Chim. Acta* **2002**, 327, 140.
 (25) Nicholson, T.; Zubieta, J. *Polyhedron* **1988**, 7, 171.
 (26) Nicholson, T.; Zubieta, J. *J. Chem. Soc., Chem. Commun.* **1985**, 367.
 (27) Xu, L.; Pierrero, J.; Patrick, B. O.; Orvig, C. *Inorg. Chem.* **2001**, 40, 2005.
 (28) Fergusson, J. E. *Coord. Chem. Rev.* **1966**, 459.

(13) O'Connor, C. J. *Prog. Inorg. Chem.* **1979**, 29, 203.

(14) Rouschais, G.; Wilkinson, G. J. *Chem. Soc. A* **1967**, 993.

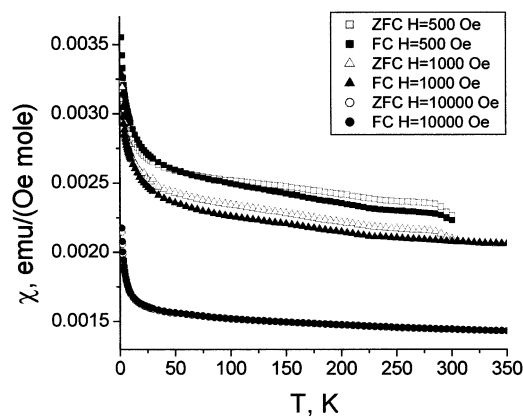


Figure 1. Dependence of magnetic susceptibility χ on temperature T for different magnetic fields H for $[\text{ReCl}_3(\text{L}^1\text{Et})]$ (**1**).

single-crystal studies would be required to resolve the influence of spin–orbit interactions for the Re(III)- d^4 center.

The magnetic behavior of Re(III) is rather complex, with different compounds exhibiting different degrees of paramagnetism and even diamagnetism.^{8,22,23,29–32} In an octahedral field, theory predicts paramagnetic behavior for Re(III). The large zero field splitting due to spin–orbit coupling for the $5d^4$ configuration implies that only low-spin complexes will exist. Since the susceptibility of **1** reflects spin–orbit interactions and the second-order Zeeman effect, the magnetic data could not be interpreted to provide a temperature-dependent moment.

In the case of compound **1**, the susceptibility varies with temperature. Such behavior is generally ascribed to the presence of impurities or exchange interactions. Since the temperature dependence of **1** does not follow the Curie law, a paramagnetic impurity can be ruled out. While the magnetization vs magnetic field dependence (Figure 2) can be explained in terms of exchange interactions, more definitive arguments cannot be made from these magnetic studies.

Despite the paramagnetism of **1**, the ^1H NMR spectrum is readily observed, as shown in Figure 3. However, since the spectrum of **1** was not readily assignable, the thiocyanate derivative $[\text{Re}(\text{NCS})_3(\text{L}^1\text{Et})]$ (**5**) was prepared as yellow crystals from the reaction of **1** with excess KSCN in acetonitrile. The paramagnetically shifted ^1H NMR spectrum of $[\text{Re}(\text{NCS})_3(\text{L}^1\text{Et})]$ (**5**), shown in Figure 4, can be reasonably explained on the basis of signal-intensity, spin-spin structure and previously reported examples of paramagnetic Re(III) NMR spectra.^{16,18,22} There are no significant chemical shift changes observed for the ester methylene and methyl protons [δ 3.48 ppm (quartet) and 0.996 ppm (triplet), respectively] and for the *N*-methylene protons (δ 2.49 ppm) adjacent to the ester group of the ligand, L^1Et . Large changes in chemical shift values for pyridyl protons arise due to the proximity of the paramagnetic Re(III) center. There are two doublets at δ 17.21 and -7.48 ppm and two triplets at δ

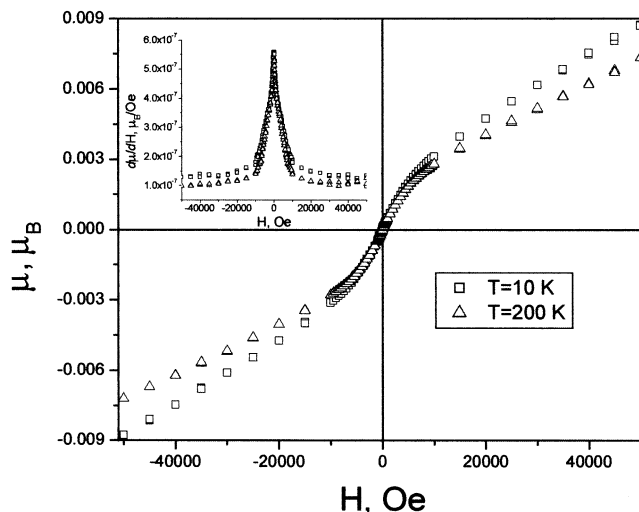


Figure 2. Dependence of magnetic moment/Re atom (μ in Bohr magnetons) on magnetic field H at 10 and 200 K. The magnetic field dependence of the magnetic susceptibility of **1** is shown in the inset.

15.35 and -6.07 ppm, with unexceptional coupling constant values, in the range 6–7.7 Hz, corresponding to one set of pyridyl protons. The sets of two doublets at δ 18.76 and 11.03 ppm with coupling constant of 18 Hz are assigned to geminal coupling of the methylene protons adjacent to the pyridyl groups of the ligand. These observations are consistent with a mirror plane bisecting the ligand C6–N1–C6A angle through the Re–N1–Cl2 plane. The X-ray structures of $[\text{ReCl}_3(\text{L}^1\text{Et})]$ (**1**) and $[\text{ReCl}_3(\text{L}^4\text{Et})]$ (**4**) confirm this analysis. Furthermore, the ^1H NMR data indicate that the complexes retain their solid-state structure in solution.

Crystallographic Studies. As shown in Figure 5, the structure of $[\text{ReCl}_3(\text{L}^1\text{Et})]$ (**1**) consists of isolated mononuclear molecular units of distorted octahedral geometry, with the chloride donors in the facial orientation. The remaining coordination sites are occupied by the amine nitrogen and two pyridine nitrogen donors of the ligand (2- $\text{C}_5\text{H}_4\text{NCH}_2$) $_2\text{NCH}_2\text{CO}_2\text{Et}$ (L^1Et). The average Re–Cl distance of 2.386(4) Å is unexceptional. The Re–N1 distance of 2.15(1) Å is significantly longer than the Re–N2 bond lengths of 2.075(9) Å, as anticipated for sp^3 hybridization at N1 and sp^2 hybridization at the N2 sites. The major angular distortions from idealized octahedral geometry are a consequence of the constraints imposed by the tridentate chelate ligand which forms five-membered rings with the rhenium center, resulting in N1–Re–N2 and N2–Re–N2 angles of 80.4(4) and 82.1(6) $^\circ$, respectively. The steric requirements of the chloride ligands result in enlargement of the Cl–Re–Cl angles to 92.7(4) $^\circ$ (average). This steric effect is also manifested in the Cl–Re–N cis angles of 92.9(4) $^\circ$ (average) and in the Cl–Re–N trans angles of 171.8(4) $^\circ$ (average). The metrical parameters associated with the $-\text{CH}_2\text{CO}_2\text{C}_2\text{H}_5$ pendant arm are unexceptional.

The structure of $[\text{ReCl}_3(\text{L}^4\text{Et})]$ (**4**), shown in Figure 6, is analogous to that of **1** with the exception that one pyridyl arm of the ligand has been replaced by a methylimidazole group. Once again the chloride donors adopt a facial orientation about the rhenium(III) center, with an average

(29) Colton, R.; Levitus, R.; Wilkinson, G. *J. Chem. Soc.* **1960**, 4121.
 (30) Colton, R.; Pearcock, R. D.; Wilkinson, G. *J. Chem. Soc.* **1960**, 1374.
 (31) Earnshaw, A.; Figgis, B. N.; Lewis, J.; Pearcock, R. D. *J. Chem. Soc.* **1961**, 3132.
 (32) McConnachie, C. A.; Stiefel, E. I. *Inorg. Chem.* **1997**, *36*, 6144.

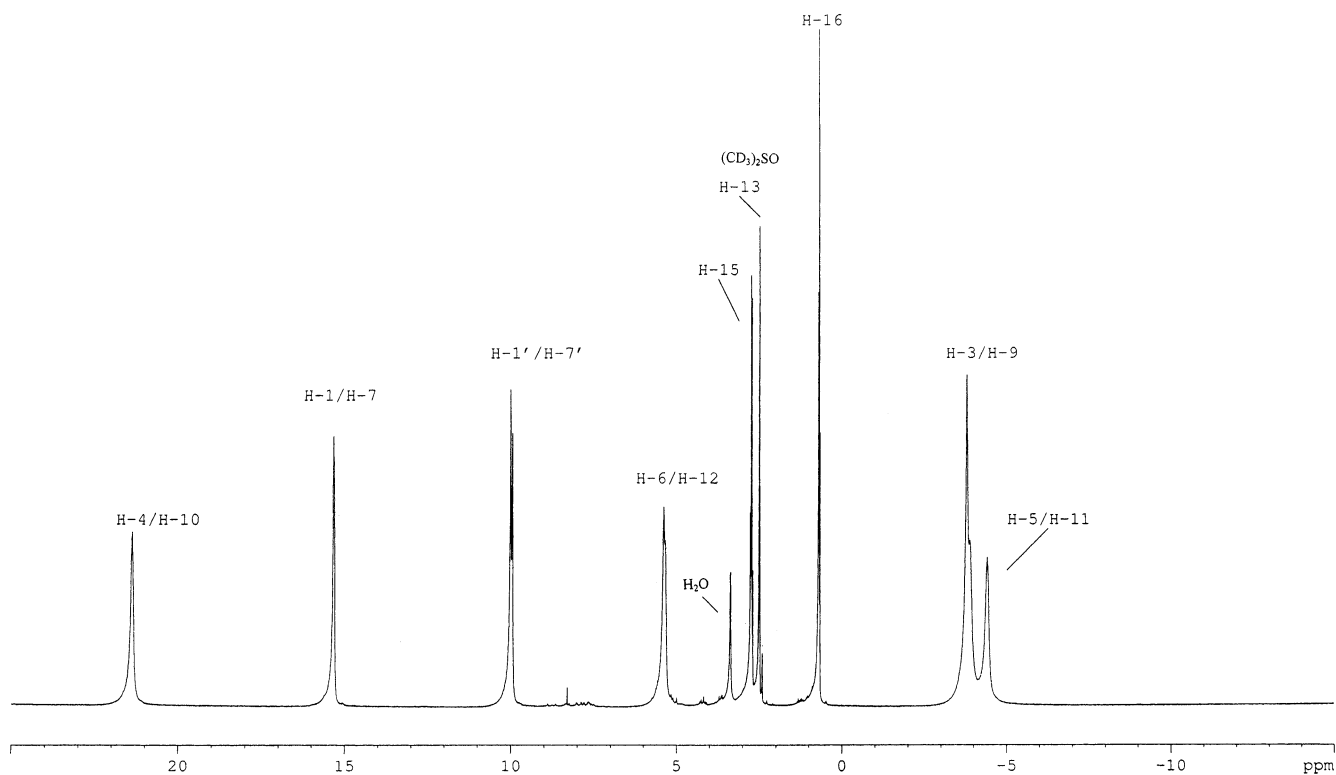


Figure 3. ¹H NMR spectrum of [ReCl₃(L¹Et)] (**1**) in (CD₃)₂SO at room temperature.

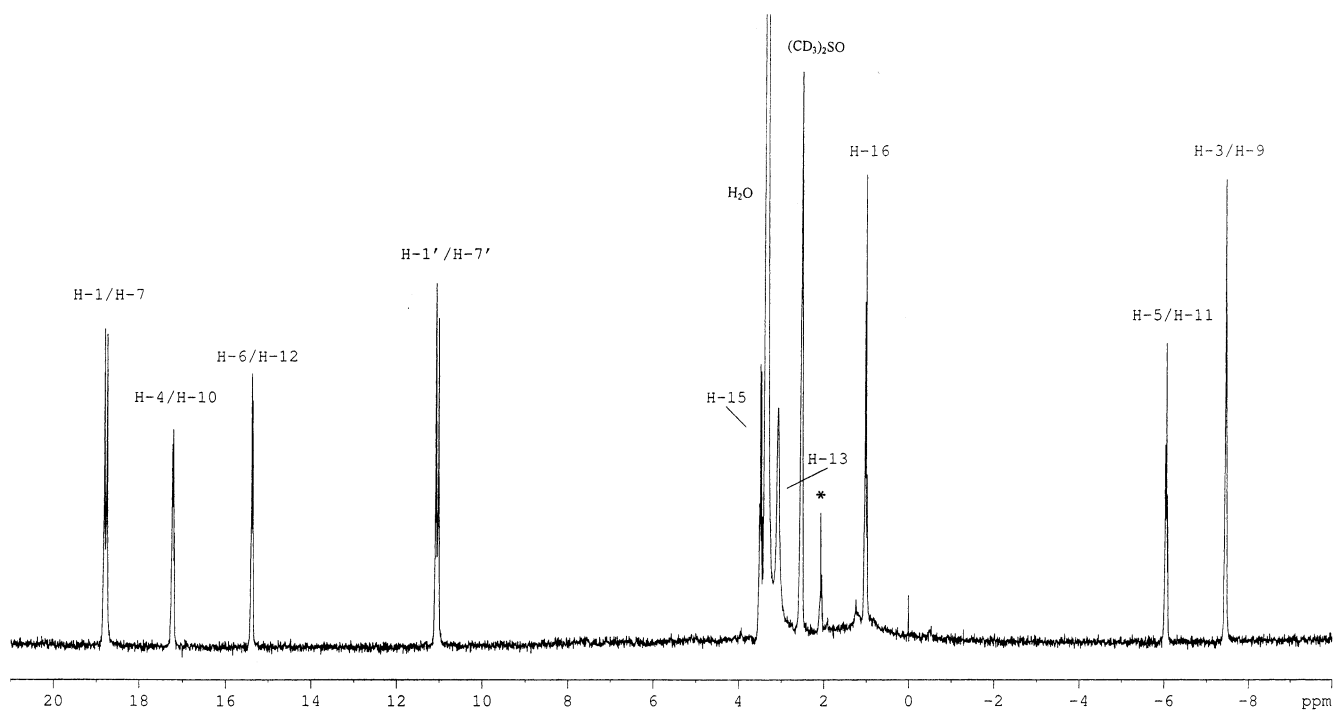


Figure 4. ¹H NMR spectrum of [Re(SCN)₃(L¹Et)] (**5**) in (CD₃)₂SO at room temperature. Unassigned peak (*) is due to a trace impurity.

Re–Cl bond distance of 2.393(2) Å. The Re–N amine distance is significantly longer at 2.209(5) Å than the Re–N pyridine and Re–N imidazole distances of 2.078(6) and 2.084(5) Å, respectively. The angular distortions from idealized octahedral geometry are similar to those observed for **1**.

Previously reported examples of the *fac*-MCl₃ core with bis(pyridylmethyl)amine-based ligands include [FeCl₃(bpa)]

(bpa = bis(2-pyridylmethyl)amine)³³ and [FeCl₃(bpe)] (bpe = ((bis(2-pyridylmethyl)amino)methyl)acetate).³⁴ The metrical parameters associated with the *fac*-{MCl₃N₃} coordination cores of these materials are similar to those of **1** and **4**.

(33) Bhattacharyya, S.; Banerjee, S.; Dirghangi, B. K.; Menon, M.; Chakravorty, A. *J. Chem. Soc., Dalton Trans.* **1999**, 155.

(34) Rodriguez, M.-C.; Lambert, F.; Morgenstern-Badarau, I. *Inorg. Chem.* **1997**, *36*, 3525.

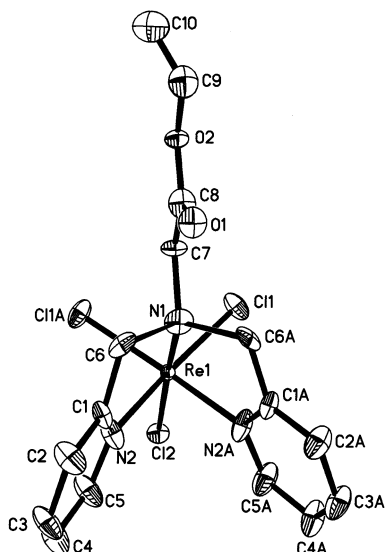


Figure 5. View of the structure of $[\text{ReCl}_3(\text{L}^1\text{Et})]$ (**1**), showing the atom-labeling scheme and 50% probability ellipsoids.

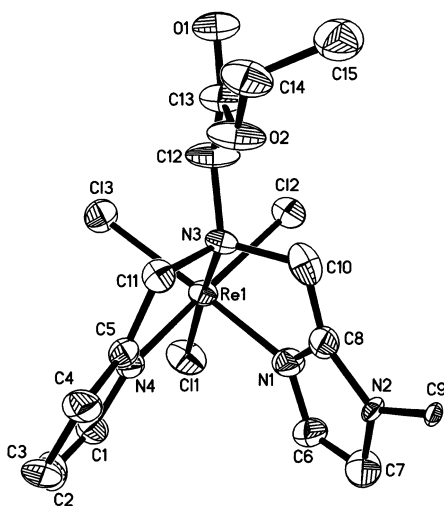


Figure 6. View of the structure of $[\text{ReCl}_3(\text{L}^4\text{Et})]$ (**4**), showing the atom-labeling scheme and 50% probability ellipsoids.

The analogous ligand (bis(2-pyridylmethyl)amino)ethane (bpea) has been described in the structure of *trans-fac*- $[\text{Re}(\text{H}_2\text{O})(\text{bpea})(\text{bpy})](\text{PF}_6)$.³⁵

Electrochemistry. The electrochemical behavior of the Re(III) complexes **1–4** was studied in acetonitrile solution using the conditions described in the Experimental Section. The complexes display two quasi-reversible (peak to peak separation 60–82 mV) one-electron couples in the ranges

of +0.021 to -0.198 V and -1.414 to -1.71 V. The electrode process near 0.0 V is assigned to the oxidation couple $\text{Re}^{\text{IV}}/\text{Re}^{\text{III}}$, and that found at potentials higher than -1.40 V is assigned as the reduction couple $\text{Re}^{\text{III}}/\text{Re}^{\text{II}}$. The oxidized complex is unstable, and it has not been possible to isolate it by coulometric experiments.

The $E_{1/2}$ values of the series **1–4** are consistent with the substituent effects. The higher $E_{1/2}$ values for complexes **1–3** compared to **4** are anticipated as a consequence of the better electron acceptor properties of $\text{L}^1\text{Et}–\text{L}^3\text{H}$ which contain pyridyl groups, in contrast to L^4Et which contains one pyridyl and one imidazolyl group.

This redox behavior is similar to that of previously reported examples of Re(IV)/Re(III) and Re(III)/Re(II) processes.^{16,18,20,33,36,37} The redox potentials of **1–4** are consistent with the correlations of Re(IV)/Re(III) and Re(III)/Re(II) couples with ligand contributions described by Lever.³⁵

Conclusions

A series of tridentate nitrogen donor ligands has been developed, starting from amino acids and amino acid analogues. The ligands react with the Re(V) starting material $[\text{ReO}(\text{PPh}_3)_2\text{Cl}_3]$ with facile displacement of the oxo group and the phosphine ligands and concomitant reduction to yield Re(III) complexes of the general type $[\text{ReCl}_3(\text{L}^n\text{R})]$. The Re(III) complexes are paramagnetic and readily oxidized to the Re(IV) species, $[\text{ReCl}_3(\text{L}^n\text{R})]^+$.

The structural studies confirm that the $\{\text{ReCl}_3\}$ core in these complexes exhibits a facial arrangement of chloride donors. The coordination sphere is completed by the nitrogen donors of the tridentate ligands, leaving a pendant arm from the central amine nitrogen available for coupling to peptides, proteins, or antibodies. The coupling of the bifunctional chelates of this study to target specific small peptides is under investigation, as well as the isolation and characterization of the ^{99}Tc radioconjugates.

Acknowledgment. This work was supported by a grant from the Department of Energy (DOE), Office of Health and Environmental Research (D2-FG02-99ER62791).

Supporting Information Available: Complete crystal data, final coordinates, temperature factors, distances, and angles for the crystallographic study of **1** and **4** in table and CIF format. This material is available free of charge via the Internet at <http://pubs.acs.org>.

IC020391D

(35) Rodriguez, M.; Romero, I.; Llobet, A.; Deronzier, A.; Biner, M.; Parella, T.; Stoeckli-Evans, H. *Inorg. Chem.* **2001**, *40*, 4150.

(36) Dilworth, J. R.; Hu, J.; Miller, J. R.; Hughes, D. L.; Zubieta, J.; Chen, Q. *J. Chem. Soc., Dalton Trans.* **1995**, 3153.

(37) Lever, A. B. P. *Inorg. Chem.* **1991**, *30*, 1980.